# Formation of oriented particles in an amorphous host: ZnS nanocrystals in silicon

A. Meldrum,[a] R. A. Zuhr, E. Sonder, J. D. Budai, C. W. White, and L. A. Boatner
*Oak Ridge National Laboratory, Solid State Division, Oak Ridge, Tennessee 37831-6057*

R. C. Ewing
*Department of NE&RS, The University of Michigan, Ann Arbor, Michigan 48109*

D. O. Henderson
*Department of Physics, Fisk University, Nashville, Tennessee 37208*

(Received 8 October 1998; accepted for publication 30 November 1998)

Processes for incorporating randomly oriented crystalline precipitates in an amorphous host can be traced back to the 17th century when Cassius produced ''gold ruby'' glass. In this glass, octahedral colloidal precipitates of gold scatter light by the Mie process to produce a deep red color. In contrast to gold ruby glass, we describe a type of material in which the crystalline precipitates are crystallographically aligned in a coherent manner—even though they are dispersed in an amorphous matrix. Ion implantation and thermal processing are first used to form zinc sulfide nanocrystals that are coherently oriented with respect to a crystalline Si host. The Si is then amorphized by ion irradiation leaving the highly radiation-resistant ZnS precipitates in an aligned crystalline state. The process is anticipated to find applications in the creation of surfaces with unique optoelectronic properties. © *1999 American Institute of Physics.* [S0003-6951(99)02905-8]

A process in which gold was used to impart an attractive deep red color to glass was discovered by Cassius around 1685.[1] Approximately 170 years later, Faraday[2] reproduced this red coloration by preparing colloidal dispersions of metallic gold particles, and more recently in 1908, Mie[3] explained the origin of the colors produced by dispersions of small particles by solving Maxwell's equations for the case of a spherical particle with a complex refractive index. The optical effects resulting from the so-called ''Mie scattering'' process depend on the size, size distribution, and shape of the nanophase particles; and there is also an early report[4] of optical effects in which the application of a magnetic or electric field to an oxide sol produced optical double refraction attributed to particle alignment.

The small particles present in the 17th century ''purple of Cassius'' and in the gold sols prepared by Faraday were randomly oriented both crystallographically and morphologically as are the nanophase particles formed in some materials by modern methods such as pulsed-laser deposition.[5] In the case of nanophase precipitates formed in single-crystal hosts, however, ion implantation combined with thermal processing has been used to form semiconducting compound crystalline precipitates that are both faceted and crystallographically aligned coherently with a host crystal lattice.[6–8] In the present work, we show that crystalline precipitates that are coherently aligned crystallographically can also be made to occur in an amorphous matrix. This is achieved by using ion implantation and thermal processing to produce ZnS nanocrystals that are coherently oriented with respect to an initially single-crystal Si host. The ZnS particles are significantly more resistant to ion irradiation-induced amorphization[9] than is the host Si matrix, and accordingly, ion bombardment with $Si^+$ ions at an appropriate fluence can subsequently be used to amorphize the Si host leaving the remaining crystalline ZnS particles in a coherently aligned state.

In this work, Si was selected as the crystalline host based on ion-irradiation experiments conducted *in situ* in a transmission electron microscope (TEM) using several potential host compositions. These included the simple oxides MgO, $Al_2O_3$, and $SiO_2$ as well as Si, $LaPO_4$, and $SrTiO_3$. The ion fluence required to induce the crystalline-to-amorphous transition was monitored for each material as a function of temperature by using electron diffraction. On this basis, the most promising host materials were found to be Si and $SrTiO_3$. Both materials could be easily amorphized at relatively low temperatures but remained crystalline above ~200 °C (see Fig. 1). Si was selected for the present experiments, however, due to its close lattice match with the ZnS zincblende structure. Additionally, Si can be readily amorphized by $Si^+$ ion irradiation thereby eliminating potential impurity effects in the host, and it also affords the opportunity for additional subsequent materials modification through the potential conversion of the Si near-surface layer into $SiO_2$ either through thermal oxidation or by oxygen implantation.

Nanophase precipitates of ZnS were formed in the near-surface region of a (100)-oriented single-crystal Si wafer by the sequential stoichiometric implantation of zinc and sulfur. The Si substrate temperature was maintained at 550 °C during the ion implantation. The ion fluence was $5\times10^{16}\,cm^{-2}$ for each element, and the ion energies were selected to give overlapping implantation profiles (i.e., 280 keV for Zn and 160 keV for S). The implanted specimens were subsequently annealed for 1 h at 1000 °C in flowing $Ar+4\%H_2$ and were then characterized using Rutherford backscattering spectroscopy (RBS), x-ray diffraction, and cross-sectional high-

[a]Electronic mail: al-m@worldnet.att.net

 

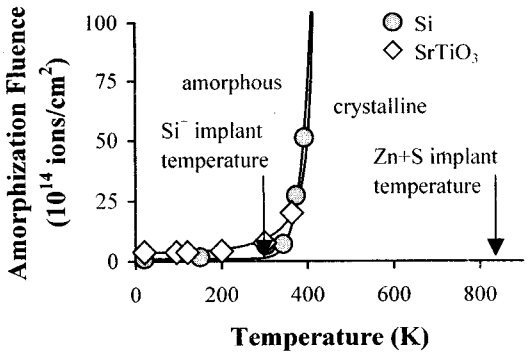


FIG. 1. Temperature dependence of the amorphization fluence for $SrTiO_3$ and Si irradiated with 800 keV $Kr^+$ ions. The ion irradiations were performed *in situ* in the HVEM Facility at Argonne National Laboratory. Both compounds can be amorphized at room temperature but cannot be amorphized above ~400 K. ZnS was not amorphized after irradiation with $10^{17}$ ions/cm$^2$ at room temperature (Ref. 9) or after $5\times10^{15}$ ions/cm$^2$ at ~100 K (in the present work). To ensure that the matrix is amorphized but not the precipitates, the irradiation temperature window is between 100 and 400 K.

resolution TEM. RBS analysis showed approximately Gaussian concentration profiles for both the Zn and S implants that were centered at a depth of ~300 nm. X-ray diffraction measurements confirmed the formation of zincblende-structure ZnS precipitates in crystalline Si, and TEM analysis revealed the presence of a band of faceted crystallographically coherent (with respect to the Si host and, accordingly with respect to each other) ZnS precipitates at a depth consistent with the RBS results (see Fig. 2).

Si wafers containing the ZnS precipitates were irradiated

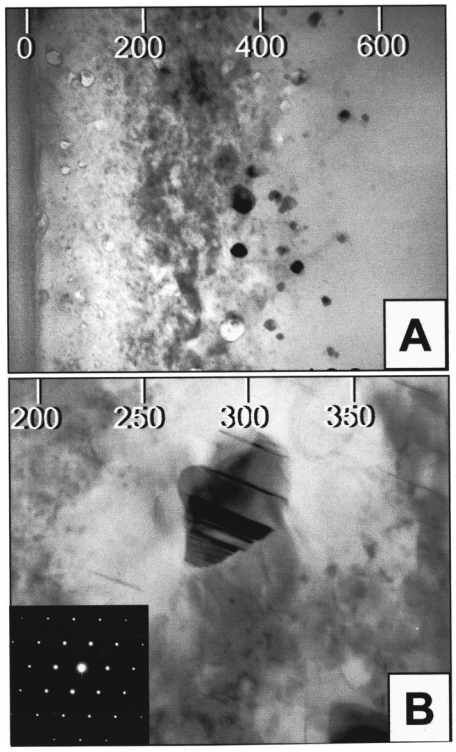


FIG. 2. (A) Cross-sectional TEM image taken 10° off the [011] zone axis showing faceted ZnS precipitates embedded in a silicon host matrix. In (B), a [011] zone-axis image highlights the twinning in a large ZnS precipitate. The corresponding electron-diffraction pattern is shown in the inset.

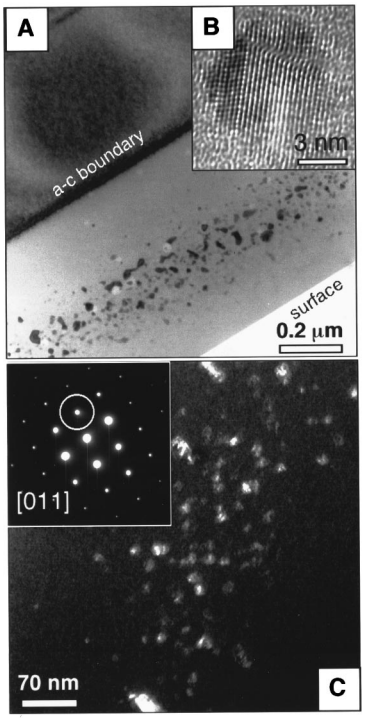


FIG. 3. (A) Cross-sectional TEM micrograph showing a band of ZnS nanocrystal precipitates centered at a depth of 250 nm. The amorphous–crystalline boundary occurs at a depth of about 750 nm. (B) High-resolution image of a ZnS nanocrystal in the amorphous Si host. The electron beam was parallel to the original [011] zone axis. The nanocrystal is crystalline, faceted, and a twin is visible as a V-shaped feature. (C) Dark field image using the Si (111) diffraction spot (circled).

at room temperature with $^{30}Si^+$ ions to a total fluence of $4.75\times10^{15}$ cm$^{-2}$, and several ion energies were used to ensure the complete amorphization of the silicon host to a depth well below the layer of ZnS nanocrystals. These irradiation conditions were selected on the basis of the results shown in Fig. 1 in order to leave the ZnS particles in a fully crystalline state following the $Si^+$ irradiation. Monte Carlo calculations[10] showed that the total amount of Si retained between the sample surface and a depth of 300 nm corresponded to less than 10 at. %, and therefore, the effect of implanted Si impurities on the ZnS precipitates should be relatively small.

Cross-sectional TEM analysis of the samples [Fig. 3(a)] following the Si irradiation clearly showed that the ZnS nanoparticles remained intact during the irradiation (i.e., the particles did not disintegrate as has been observed previously in the case of gold nanoparticles in $SiO_2$),[11] nor was there any evidence of ion-beam mixing into the Si host. The TEM results showed that the Si crystalline–amorphous boundary was at a depth of 700 nm—well beyond the layer of ZnS nanocrystals. Figure 3(b) shows a lattice-fringe image of a single ZnS nanocrystal embedded in the amorphous Si host. The ZnS particle is crystalline, faceted, and in this example, twinned. Lattice fringes observed for the other ZnS particles were similarly oriented, establishing that a new type of near-surface nanocomposite has been formed that consists of crystallographically oriented, dispersed precipitates in an amorphous host matrix. Figure 3(c) shows a dark-field image formed with a (111) diffracted beam. The ZnS nanocrystals simultaneously diffract into this beam, and hence, appear

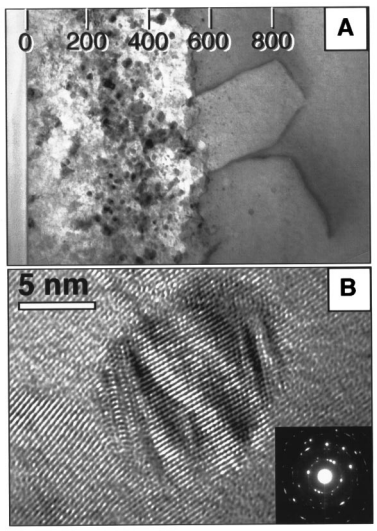


FIG. 4. (A) Cross-sectional TEM micrograph showing the specimen in Fig. 3 after annealing at 575 °C for 90 min. An irregular boundary formed at a depth of 530 nm. ZnS nanocrystals occur in the indents of this boundary. Some pinning dislocations are observed as dark lines in the epitaxially crystallized layer below this boundary. (B) A single ZnS nanocrystal showing Moiré fringe contrast. The Si host is polycrystalline, as indicated by the diffraction pattern (inset).

bright—providing clear evidence for the coherently oriented crystalline nature of the particles.

The microstructural evolution of the ZnS/amorphous Si layer due to thermally induced solid-phase epitaxial recrystallization of the Si host was also investigated. Of fundamental interest in these studies was the effect of the ZnS particles on the amorphous–crystalline Si boundary as it passed the crystalline precipitates during the regrowth process. Recrystallization of the amorphous ZnS particle-containing Si layer was achieved by annealing the samples for 90 min at 575 °C in flowing $Ar+4\%H_2$. An ion-beam amorphized Si specimen that did not contain the ZnS precipitates was also annealed as a control sample. An analysis of this control specimen confirmed that the recrystallization process was completed under the conditions noted (i.e., there was no remaining amorphous material). Additionally, pinning dislocations were present in this sample that accounted for the residual scattering yield observed in RBS-channeling spectra. In the case of the sample containing the crystalline ZnS precipitates, epitaxial recrystallization of the amorphous Si layer occurred only up to the beginning of the ZnS particle layer [see Fig. 4(a)]. Pinning dislocations were also present in this initial epitaxially regrown layer. As the crystalline–amorphous boundary initially approached the ZnS precipitates, an irregular interface began to form with the ZnS particles located in ''indents'' in the boundary region. The Si recrystallization boundary was subsequently only able to partially envelope the ZnS particles before losing its crystalline coherence relative to the underlying bulk crystalline Si. In Fig. 4(b), a high-resolution image of an embedded ZnS nanocrystal shows the discontinuous nature of the recrystallized Si host material. Nevertheless, the relative crystallographic orientation of the ZnS nanoparticles was still retained throughout the Si regrowth process and effectively provided a ''marker'' for the original orientation of the Si host.

The unique physical, magnetic, optical, and electronic properties of nanocrystalline materials have been established in numerous recent investigations and many of these properties represent the basis for potentially important device applications. In the particular case of semiconducting nanocrystals, such as the ZnS precipitates investigated here, electron localization (quantum confinement) effects can lead to band gap, absorption, and luminescence tunability as a function of particle size.[12] These optical effects as well as other physical and electronic effects depend not only on the size and size distribution of the nanocrystals but on nanocrystal–host interactions as well. By exploiting the flexibility of ion implantation and the intrinsic differences in the recrystallization behavior between potential host materials and various types of nanophase precipitates, it should be possible to achieve a wide range of surface nanocomposite systems consisting of various types of oriented crystalline particles embedded in a variety of amorphous matrices. It is anticipated that new effects associated with the crystallographic and/or morphological particulate orientation will be found in surface nanocomposite systems of this type.

One of the authors (A.M.) acknowledges support from the Natural Sciences and Engineering Research Council of Canada. Oak Ridge National Laboratory is managed by Lockheed Martin Energy Research Corp. for the U.S. Department of Energy under Contract No. DE-AC05-96OR22464.

[1] R. J. Charleston, *Masterpieces of Glass: A World History from the Corning Museum of Glass* (Harry N. Abrams, New York, 1990).
[2] M. Faraday, Proc. R. Soc. London **8**, 356 (1857).
[3] G. Mie, Ann. Phys. (Leipzig) **25**, 25 (1908).
[4] Majorana, Atti Accad. Naz. Lincei, Cl. Sci. Fis. Mat. Nat. Rend. **11**, 374 (1902).
[5] J. M. Ballesteros, R. Serna, J. Solis, C. N. Alfonso, A. K. Petford-Long, D. H. Osborne, and R. F. Haglund, Appl. Phys. Lett. **71**, 2445 (1997).
[6] C. W. White, J. D. Budai, S. P. Withrow, J. G. Zhu, E. Sonder, R. A. Zuhr, A. Meldrum, D. M. Hembree, D. O. Henderson, and S. Prawer, Nucl. Instrum. Methods Phys. Res. B **141**, 228 (1998).
[7] J. D. Budai, C. W. White, S. P. Withrow, M. F. Chisholm, J. Zhu, and R. A. Zuhr, Nature (London) **390**, 384 (1997).
[8] A. Meldrum, C. W. White, L. A. Boatner, I. M. Anderson, R. A. Zuhr, E. Sonder, J. D. Budai, and D. O. Henderson, Nucl. Instrum. Methods Phys. Res. (in press).
[9] H. M. Naguib and R. Kelly, Radiat. Eff. **25**, 1 (1975).
[10] J. F. Zeigler, *Transport and Range of Ions in Matter* (TRIM) *Version 96* (IBM Research, Yorktown, NY, 1996).
[11] C. W. White (unpublished data).
[12] P. Alivisatos, Science **271**, 933 (1996).